applied optics

Carrier-envelope phase stable, 5.4 μJ, broadband, mid-infrared pulse generation from a 1-ps, Yb:YAG thin-disk laser

Ayman Alismail,[1,2] Haochuan Wang,[1,3] Najd Altwaijry,[1,2] and Hanieh Fattahi[1,3,*]

[1]Department für Physik, Ludwig-Maximilians-Universität München, Am Coulombwall 1, D-85748 Garching, Germany
[2]Physics and Astronomy Department, King Saud University, Riyadh 11451, Saudi Arabia
[3]Max-Planck Institut für Quantenoptik, Hans-Kopfermann-Str. 1, D-85748 Garching, Germany
*Corresponding author: hanieh.fattahi@mpq.mpg.de

Received 14 April 2017; revised 18 May 2017; accepted 19 May 2017; posted 19 May 2017 (Doc. ID 292848); published 9 June 2017

We report on a simple scheme to generate broadband, μJ pulses centered at 2.1 μm with an intrinsic carrier-envelope phase (CEP) stability from the output of a Yb:YAG regenerative amplifier delivering 1-ps pulses with randomly varying CEP. To the best of our knowledge, the reported system has the highest optical-to-optical efficiency for converting 1-ps, 1 μm pulses to CEP stable, broadband, 2.1 μm pulses. The generated coherent light carries an energy of 5.4 μJ, at 5 kHz repetition rate, that can be scaled to higher energy or power by using a suitable front end, if required. The system is ideally suited for seeding broadband parametric amplifiers and multichannel synthesizers pumped by picosecond Yb-doped amplifiers, obviating the need for active timing synchronization. Alternatively, this scheme can be combined with high-power oscillators with tens of μJ energy to generate CEP stable, multioctave supercontinua, suitable for field-resolved and time-resolved spectroscopy.

OCIS codes: (140.3615) Lasers, ytterbium; (190.4223) Nonlinear wave mixing; (320.7110) Ultrafast nonlinear optics; (190.4380) Nonlinear optics, four-wave mixing; (140.7090) Ultrafast lasers.

https://doi.org/10.1364/AO.56.004990

1. INTRODUCTION

In femtosecond spectroscopy, the effect of a pump pulse on the envelope of a delayed probe pulse is measured, leaving effects occurring in response to the oscillating electric field unresolved [1]. On longer time scales, the polarization of a medium, in both amplitude and phase, could be retrieved from a measurement of the oscillating electric field of picosecond terahertz pulses that propagate through the medium. Access to this full polarization response, however, does rely on a gate pulse much shorter than the field cycle. This requirement had prevented the extension of the technique into the optical regime, due to the absence of sampling pulses shorter than the oscillation period of visible (VIS) or near-infrared light.

In the last decade, Ti:Sa laser technology enabled generation of coherent extreme-ultraviolet (XUV) pulses with attosecond duration and changed this scenario. Scanning the synchronized XUV pulses relative to their VIS driver pulses allowed the measurement of the light's electric field at petahertz frequencies [2]. Following recent advancement of Yb:YAG-pumped optical parametric amplifiers, field-resolved detection at kilohertz repetition rates has been extended to mid-infrared (MIR) by employing electro-optic sampling, wherein VIS, few-cycle pulses were used as a probe [3]. Field detection based on electro-optic sampling can provide a better understanding of extremely fast dynamics in solid-state materials [4] and benefits from few-cycle pulses in MIR and VIS spectral range, with carrier-envelope-phase (CEP) stability and at high repetition rates.

These applications call for compact sources, delivering CEP stable, coherent, superoctave continua spanning from VIS to MIR spectral range, beyond nanojoule energy, and at kilohertz to megahertz repetition rates. Today, Yb:YAG lasers are mature, turnkey, and cost-effective technology, and offer such a possibility [5–12].

Specifically, a CEP stable, multioctave supercontinuum generated directly from Yb:YAG, sub-ps oscillators or ps amplifiers has two prominent applications: (I) it can be used to seed broadband optical parametric amplifiers (OPAs) or subcycle field synthesizers pumped by high-energy, kHz, Yb:YAG amplifiers [5,13,14], obviating the need for complex temporal synchronization systems between two independent lasers [15,16]; or, it can be used for (II) field- and time-resolved spectroscopy when it is driven from high average-power, MHz oscillators.

MIR superoctave continua have been generated from randomly phased Yb:YAG lasers, by combining supercontinuum

generation in bulk and difference frequency generation [17,18], or by using high-energy, CEP stable MIR pulses from an OPA [19–21] and spectrally broaden them in bulk, gas, or a gas-filled hollow-core fiber [22–24]. Such supercontinua are generated in systems with very low conversion efficiency, containing several nonlinear stages and mostly with a need for an additional complex temporal synchronization stage.

In this paper, we demonstrate an efficient scheme to generate broadband, CEP stable, MIR pulses directly from a ps-long Yb:YAG, thin-disk laser at 5 kHz repetition rate. To the best of our knowledge, this system has the highest reported optical-to-optical efficiency for converting ps-long pulses at 1030 nm with randomly varying phase, to broadband, CEP stable pulses at 2.1 μm. This critical property makes this setup compatible to the output parameters of high-power, low-energy, Yb:YAG oscillators [25,26] keeping the promise to generate a CEP stable, VIS-MIR supercontinuum at MHz repetition rates to extend the filed-resolved spectroscopy [4] to a MIR spectral range.

2. EXPERIMENTAL SETUP

The experimental setup is illustrated in Fig. 1. A Yb:YAG thin-disk regenerative amplifier delivering 20 mJ, 1-ps pulses at 5 kHz repetition rate [27] is used as the front end of the system. 400 μJ of the total energy of the amplifier is separated by using an attenuator consisting of a thin-film polarizer (TFP) and a $\lambda/2$-plate, and are then frequency doubled in a 1.5-mm-thick, type-I, beta barium borate (BBO) crystal at the phase matching angle of 23°.

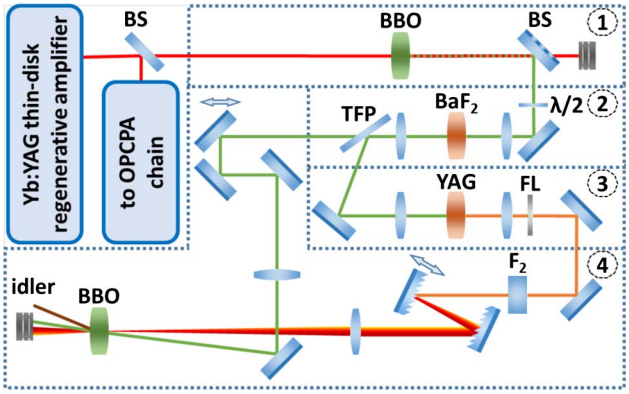

Fig. 1. Schematic of the setup to convert 400 μJ of a 1-ps, 20 mJ Yb:YAG, thin-disk amplifier to carrier-envelope phase stable, broadband, 5.4 μJ pulses centered at 2.1 μm. At first, the 1-ps pulses are frequency doubled in a 1.5-mm-thick BBO crystal (block 1). Then the 260 μJ second harmonic beam is focused into a 4-mm-thick BaF_2 crystal for cross-polarized wave generation (XPW) (block 2). The 466-fs-long XPW pulses are separated from the residual energy by means of a thin-film polarizer (block 2) and focused into a 10-mm-thick plate of YAG for supercontinuum generation (block 3). The Stokes wing of the supercontinuum, centered at 680 nm, is filtered by using a 600 nm longpass filter to serve as a seed for a noncollinear optical parametric amplifier (NOPA). The seed pulses are sent through a grating pair and a 115-mm-thick F_2 to adjust their angular chirp and temporal duration. Finally the seed and pump pulses are sent to a NOPA containing a 6-mm-thick BBO crystal (block 4) to generate broadband idler pulses at 2.1 μm. BS, beam splitter; TFP, thin-film polarizer; FL, filter.

The beam size on the crystal is adjusted to reach a peak intensity of 80 GW/cm^2, and an energy of 260 μJ at 515 nm, corresponding to 65% optical-to-optical conversion efficiency, is achieved. The frequency doubling of the input pulses is necessary to ensure intrinsic CEP stability of the generated MIR pulses in the last nonlinear stage of the setup, which contains a noncollinear optical parametric amplifier (NOPA) [28].

The second harmonic (SH) pulses are temporally shortened compared to the fundamental laser pulses at 1030 nm, due to pulse shortening based on the χ^2 effect (see Ref. [27] for details). Afterward, the SH beam is focused into a 4-mm-thick BaF_2 crystal for cross-polarized wave generation (XPW) and additional pulse shortening. The 466-fs-long XPW pulses are separated from the residual SH pulses by a thin-film polarizer and focused in a bulk for supercontinuum generation in VIS frequencies [29]. This step is necessary to achieve a stable and reproducible supercontinuum [17,30]. Finally, the Stokes wing of the generated supercontinuum and the residual SH pulses are focused into a NOPA stage to generate broadband, CEP stable pulses in the MIR.

In our previous report for generating CEP stable MIR pulses [17], the supercontinuum signal was sent through two optical parametric amplifier stages: first, to amplify and stabilize the signal energy via a NOPA, and, second, to CEP stabilize and shift the idler's central frequency to the MIR in a collinear OPA. In the current MIR pulse generation setup, the nonlinear processes are reduced by combining these two parametric amplification stages into a single, saturated NOPA stage. However, in a NOPA due to the required noncollinear geometry for a broadband and efficient amplification, the generated idler inherits an angular dispersion, which must be compensated for. We chose to compensate for this angular chirp by prechirping the input seed pulses to the NOPA by means of a grating pair, motivated by the higher efficiency of grating pairs in VIS frequencies.

In what follows, detailed discussion of each block of the setup is presented.

A. XPW and Supercontinuum Driven by High-Energy Photons

It has been challenging to generate a supercontinuum using high-energy photons [31,32]. As the energy of the driving photons approaches the bandgap of transparent materials the probability of damage due to nonlinear absorption increases. In addition, the damage threshold intensity for transparent materials increases in proportion to the inverse of the square root of the pulse duration for pulsed lasers, following the dynamics of impact ionization.

Therefore, we used the XPW process to temporally shorten the driving pulses prior to the supercontinuum generation stage due to its simplicity and self-compression, which obviates the need for any additional pulse compressor. It is known that the conversion efficiency of an XPW process is proportional to the input frequency of the driving pulses, due to the increase in nonlinearity of materials when interacting with higher-energy photons [33]. However, for driving pulses with higher photon energies saturation occurs earlier, due to the dephasing between the driving pulses and the XPWs, limiting the conversion efficiency.

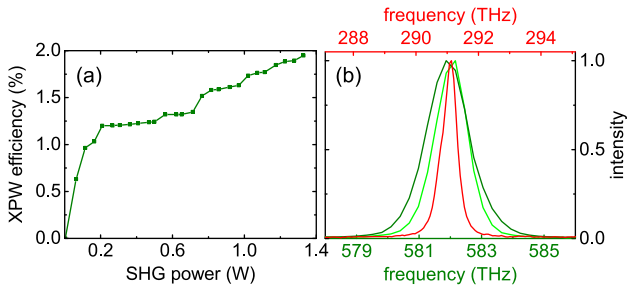

Fig. 2. (a) Optical-to-optical efficiency of the generated cross-polarized wave versus the power of the driving pulses (second harmonic pulses). (b) Normalized spectra of the fundamental (red curve), second harmonic (light green curve), and the generated cross-polarized (dark green curve) pulses with the spectral bandwidth of 0.62 THz, 1.26 THz, and 1.64 THz (FWHM), respectively.

260 μJ pulses at 515 nm are used to generate XPW in a 4-mm-thick BaF_2 crystal with a holographic cut. An $f = 150$ mm convex lens is used to focus the beam, while the crystal is placed after the focus. The beam size at the crystal is 260 μm at FWHM. Figure 2 shows the optical-to-optical conversion efficiency and the spectrum of the converted SH pulses to XPW pulses. Maximum efficiency of 2%, corresponding to 5 μJ, is achieved. Higher peak intensity on the crystal leads to its optical damage. The generated XPW pulses and the residual SH pulses are both collimated by using an $f = 150$ mm convex lens. A TFP is used to separate them afterward, as the XPW and SH beams have a crossed polarization. XPW pulses were characterized by using a cross-correlation frequency-resolved optical gating (XFROG) employing a 100-μm-thick BBO crystal. The Fourier transform limited pulses of the Yb:YAG amplifier were used as a reference pulse for the XFROG measurement. Figure 3 shows the measured and retrieved XFROG spectrograms, and the retrieved temporal profile of the XPW pulses with a 466 fs temporal duration (FWHM).

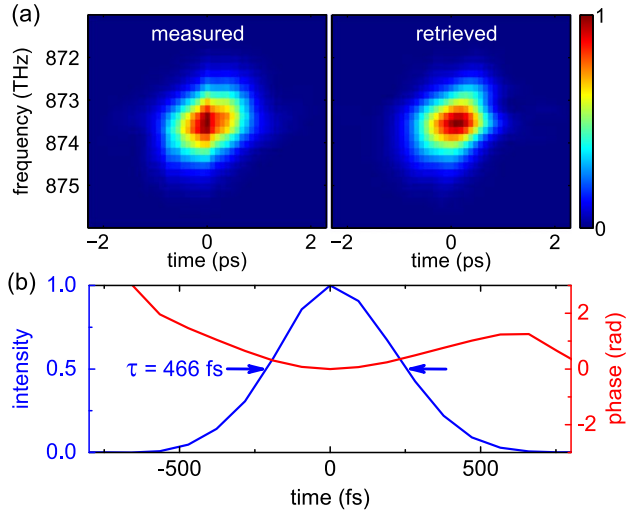

Fig. 3. Temporal profile of the generated XPW pulses at 515 nm. (a) Measured and retrieved XFROG spectrograms. (b) Retrieved temporal profile of the XPW pulses with 466 fs pulse duration at FWHM ($G_{error} = 0.01544$).

Table 1. Performance of Different Materials for Supercontinuum Generation Driven by 466 fs, 515 nm Pulses

Crystal	Thickness (mm)	Critical Power (MW)	Band Gap (eV)	Filament
YAG	2	0.22	6.3	Yes
Sapphire	2	0.68	9.9	No
TGG	4	0.12	—	No
ZnS	5	0.32	3.911	No

Thereafter, XPW pulses are focused by an $f = 125$ mm convex lens into a nonlinear medium for supercontinuum generation. We tried several nonlinear media and could achieve a stable filament only in a 2-mm-thick plate of YAG due to its lower critical power. This study is summarized in Table 1. In the final setup we chose a 10-mm-thick plate of YAG due to the better daily reproducibility.

Figure 4 shows the spectrum and the transverse beam profile of the generated supercontinuum in 10-mm-thick YAG. The anti-Stokes and Stokes wings of the supercontinuum are measured behind a 500 nm shortpass filter (FES0500, Thorlabs GmbH) and a 550 nm longpass filter (FEL0550, Thorlabs GmbH), respectively. Both wings are normalized to one separately. With a tighter focusing, a stable filament could be generated by using only 0.7 μJ energy and an $f = 40$ mm convex lens. However, we opt for generating a stable, single filament with the maximum pulse energy, by a careful balance between the beam size and the energy of the driving pulses. The Stokes wing of the supercontinuum is filtered out by a 600 nm longpass filter (FEL0600, Thorlabs GmbH) and is collimated by an $f = 125$ mm convex lens and used to seed the NOPA stage.

B. Idler Generation

To generate broadband MIR pulses, the unconverted portion of SH pulses after the XPW process are mixed with the Stokes wing of the supercontinuum in a NOPA. As described earlier, the generated idler in the noncollinear geometry has an angular chirp that can be compensated by matching the seed pulse-front to the idler pulse-front or to the propagation direction

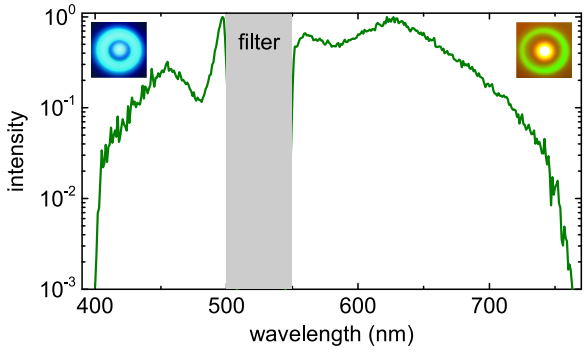

Fig. 4. Normalized spectrum and transverse beam profiles (inset) of the generated supercontinuum in 10-mm-thick YAG. The spectrum and the beam profile of the anti-Stokes and Stokes wings are measured behind a 500 nm shortpass filter and a 550 nm longpass filter, respectively.

of the idler. For ps-long pump pulses the effect of the pulse-front is negligible and can be ignored. We chose to precompensate for this angular chirp by angularly dispersing the seed pulses of the NOPA, using an aluminum-coated reflective grating pair with 300 groves/mm (GR50-0310, Thorlabs GmbH) [34,35]. We avoided using a Brewster prism pair due to its undesired higher-order dispersion.

The separation between the gratings determines the applied angular dispersion to the seed. Therefore, one of the gratings is mounted on a translation stage for adjusting the distance. Afterward the angularly chirped seed pulses are amplified in a 6-mm-thick, type-I, BBO crystal with an internal noncollinear angle of 2.4° and the phase matching angle of 23.4°. The pump and seed beams are focused down to 650 μm (FWHM) and overlapped spatially and temporally in the BBO crystal.

When the distance of the grating pair is set to 175 mm, 220 μrad/nm angular chirp is introduced to the seed pulses and an angular-chirp-free idler is generated. However, in addition to the angular chirp, the grating pair also temporally chirps the seed pulses. As a result, the seed pulses become longer than the pump pulses in the NOPA and the amplified spectral bandwidth decreases. The group delay dispersion (GDD), induced by the grating pair on the seed pulses, is calculated from Eq. (1):

$$\mathrm{GDD} = -\frac{\lambda^3 b}{2\pi c^2 d^2 \cos^3(\beta)}, \tag{1}$$

where λ, c, d, b, and β are the central wavelength of the pulse, velocity of light, grating's line density, grating separation, and diffraction angle of the grating, respectively.

Therefore, a 115-mm-thick plate of F_2 is placed in the seed beam path to compensate for the calculated, negative chirp on the seed pulses and to adjust the temporal duration of the seed pulses within the temporal window of pump pulses at the NOPA stage. The generated chirp-free idler pulses have similar temporal duration to the seed pulses, as their generation occurs only in the region that pump and seed pulses are temporally overlapped. The amplified spectrum, the idler spectrum, and the transverse spatial profile of the 5.4 μJ generated broadband chirp-free idler in the far-field are shown in Fig. 5.

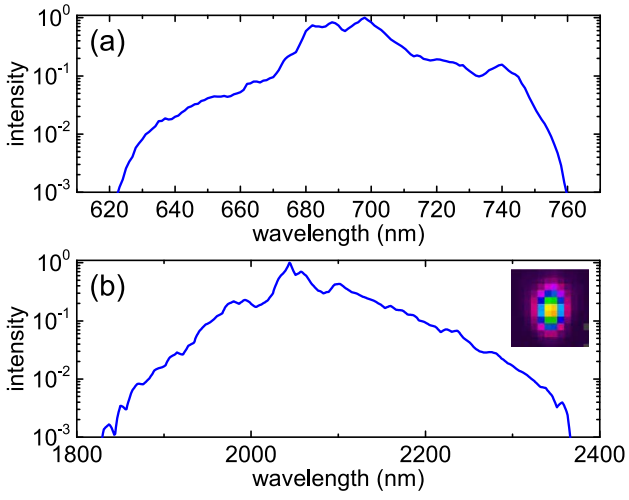

Fig. 5. (a) Normalized spectrum of the amplified seed pulses in the NOPA containing a 6-mm-thick BBO crystal. (b) Normalized spectrum of the generated chirp-free idler supporting 37 fs (FWHM) Fourier transform limited pulses. Inset: the transverse spatial profile of the generated idler at the focus.

3. CONCLUSION AND OUTLOOK

We demonstrated a compact and efficient scheme to generate broadband, CEP stable pulses at 2.1 μm, driven from a 1-ps, Yb:YAG thin-disk amplifier. The broadband MIR pulses span from 1.83 μm to 2.36 μm and contain 5.4 μJ energy. It is expected that the delivered pulses from the current system show a similar long-term, CEP stability like the previously reported work [17].

Careful design of the system led to 1.35% optical-to-optical efficiency, which is defined as the ratio of the total output pulse energy of the system to the total input pulse energy to the system. To the best of our knowledge, this is the highest reported efficiency for similar systems [17,18,34,35].

The μJ, MIR pulses can be used for CEP stable, supercontinuum generation in bulk [17,18,36], or hollow-core photonic crystal fibers [37], and can serve as an ideal front end for broadband OPAs or field synthesizers, simplifying the state of the art and obviating the need for complex temporal synchronization between pump and seed sources [15,16].

As discussed in Section 2.A, the energy threshold for generating a supercontinuum driven by 466-fs-long, 515 nm pulses is 0.7 μJ. Therefore, the required input energy to the system can be scaled down to tens of μJ. Considering this margin, it can be simply calculated that the required input peak power to achieve a CEP stable supercontinuum at the output of the setup is compatible to the peak power delivered by high average-power oscillators such as [25].

The opportunity of generating a superoctave, CEP stable continuum directly from high average-power, low peak-power sources paves the way for a new generation of lasers, suitable for femtosecond field- and time-resolved spectroscopy in the MIR spectral range.

Funding. Centre for Advanced Laser Applications (CALA).

Acknowledgment. We thank Ferenc Krausz and Maximilian Wendl for their support.

REFERENCES

1. A. H. Zewail, "Femtochemistry: atomic-scale dynamics of the chemical bond," J. Phys. Chem. A **104**, 5660–5694 (2000).
2. M. Hentschel, R. Kienberger, C. Spielmann, G. A. Reider, N. Milosevic, T. Brabec, P. Corkum, U. Heinzmann, M. Drescher, and F. Krausz, "Attosecond metrology," Nature **414**, 509–513 (2001).
3. S. Keiber, S. Sederberg, A. Schwarz, M. Trubetskov, V. Pervak, F. Krausz, and N. Karpowicz, "Electro-optic sampling of near-infrared waveforms," Nat. Photonics **10**, 159–162 (2016).
4. A. Sommer, E. M. Bothschafter, S. A. Sato, C. Jakubeit, T. Latka, O. Razskazovskaya, H. Fattahi, M. Jobst, W. Schweinberger, V. Shirvanyan, V. S. Yakovlev, R. Kienberger, K. Yabana, N. Karpowicz, M. Schultze, and F. Krausz, "Attosecond nonlinear polarization and light-matter energy transfer in solids," Nature **534**, 86–90 (2016).
5. H. Fattahi, H. G. Barros, M. Gorjan, T. Nubbemeyer, B. Alsaif, C. Y. Teisset, M. Schultze, S. Prinz, M. Haefner, M. Ueffing, A. Alismail, L. Vámos, A. Schwarz, O. Pronin, J. Brons, X. T. Geng, G. Arisholm, M. Ciappina, V. S. Yakovlev, D.-E. Kim, A. M. Azzeer, N. Karpowicz, D. Sutter, Z. Major, T. Metzger, and F. Krausz, "Third-generation femtosecond technology," Optica **1**, 45–63 (2014).

6. O. H. Heckl, J. Kleinbauer, D. Bauer, S. Weiler, T. Metzger, and D. H. Sutter, "Ultrafast thin-disk lasers," in *Ultrashort Pulse Laser Technology* (2016), pp. 93–115.
7. L. E. Zapata, H. Lin, A.-L. Calendron, H. Cankaya, M. Hemmer, F. Reichert, W. R. Huang, E. Granados, K.-H. Hong, and F. X. Kärtner, "Cryogenic Yb:YAG composite-thin-disk for high energy and average power amplifiers," Opt. Lett. **40**, 2610–2613 (2015).
8. M. Schulz, R. Riedel, A. Willner, T. Mans, C. Schnitzler, P. Russbueldt, J. Dolkemeyer, E. Seise, T. Gottschall, S. Hädrich, S. Duesterer, H. Schlarb, J. Feldhaus, J. Limpert, B. Faatz, A. Tünnermann, J. Rossbach, M. Drescher, and F. Tavella, "Yb:YAG Innoslab amplifier: efficient high repetition rate subpicosecond pumping system for optical parametric chirped pulse amplification," Opt. Lett. **36**, 2456–2458 (2011).
9. F. Röser, T. Eidam, J. Rothhardt, O. Schmidt, D. N. Schimpf, J. Limpert, and A. Tünnermann, "Millijoule pulse energy high repetition rate femtosecond fiber chirped-pulse amplification system," Opt. Lett. **32**, 3495–3497 (2007).
10. P. Russbueldt, T. Mans, G. Rotarius, J. Weitenberg, H. D. Hoffmann, and R. Poprawe, "400 W Yb:YAG innoslab fs-amplifier," Opt. Express **17**, 12230–12245 (2009).
11. C. Baumgarten, M. Pedicone, H. Bravo, H. Wang, L. Yin, C. S. Menoni, J. J. Rocca, and B. A. Reagan, "1 J, 05 kHz repetition rate picosecond laser," Opt. Lett. **41**, 3339–3342 (2016).
12. J. Novák, J. T. Green, T. Metzger, T. Mazanec, B. Himmel, M. Horáček, Z. Hubka, R. Boge, R. Antipenkov, F. Batysta, J. A. Naylon, P. Bakule, and B. Rus, "Thin disk amplifier-based 40 mJ, 1 kHz, picosecond laser at 515 nm," Opt. Express **24**, 5728–5733 (2016).
13. O. D. Mucke, S. Fang, G. Cirmi, G. M. Rossi, S.-H. Chia, H. Ye, Y. Yang, R. Mainz, C. Manzoni, P. Farinello, G. Cerullo, and F. X. Kartner, "Toward waveform nonlinear optics using multimillijoule sub-cycle waveform synthesizers," IEEE J. Sel. Top. Quantum Electron. **21**, 1–12 (2015).
14. Y. Yin, A. Chew, X. Ren, J. Li, Y. Wang, Y. Wu, and Z. Chang, "Towards terawatt sub-cycle long-wave infrared pulses via chirped optical parametric amplification and indirect pulse shaping," Sci. Rep. **7**, 45794 (2017).
15. H. Fattahi, C. Teisset, O. Pronin, A. Sugita, R. Graf, V. Pervak, X. Gu, T. Metzger, Z. Major, F. Krausz, and A. Apolonski, "Pump-seed synchronization for MHz repetition rate, high-power optical parametric chirped pulse amplification," Opt. Express **20**, 9833–9840 (2012).
16. A. Schwarz, M. Ueffing, Y. Deng, X. Gu, H. Fattahi, T. Metzger, M. Ossiander, F. Krausz, and R. Kienberger, "Active stabilization for optically synchronized optical parametric chirped pulse amplification," Opt. Express **20**, 5557–5565 (2012).
17. H. Fattahi, H. Wang, A. Alismail, G. Arisholm, V. Pervak, A. M. Azzeer, and F. Krausz, "Near-PHz-bandwidth, phase-stable continua generated from a Yb:YAG thin-disk amplifier," Opt. Express **24**, 24337–24346 (2016).
18. H. Çankaya, A.-L. Calendron, C. Zhou, S.-H. Chia, O. D. Mücke, G. Cirmi, and F. X. Kärtner, "40-μJ passively CEP-stable seed source for ytterbium-based high-energy optical waveform synthesizers," Opt. Express **24**, 25169–25180 (2016).
19. Y. Deng, A. Schwarz, H. Fattahi, M. Ueffing, X. Gu, M. Ossiander, T. Metzger, V. Pervak, H. Ishizuki, T. Taira, T. Kobayashi, G. Marcus, F. Krausz, R. Kienberger, and N. Karpowicz, "Carrier-envelope-phase-stable, 1.2 mJ, 1.5 cycle laser pulses at 2.1 μm," Opt. Lett. **37**, 4973–4975 (2012).
20. Y. Yin, J. Li, X. Ren, K. Zhao, Y. Wu, E. Cunningham, and Z. Chang, "High-efficiency optical parametric chirped-pulse amplifier in BiB_3O_6 for generation of 3 mJ, two-cycle, carrier-envelope-phase-stable pulses at 17 μm," Opt. Lett. **41**, 1142–1145 (2016).
21. C.-J. Lai, K.-H. Hong, J. P. Siqueira, P. Krogen, C.-L. Chang, G. J. Stein, H. Liang, P. D. Keathley, G. Laurent, J. Moses, L. E. Zapata, and F. X. Kärtner, "Multi-mJ mid-infrared kHz OPCPA and Yb-doped pump lasers for tabletop coherent soft x-ray generation," J. Opt. **17**, 094009 (2015).
22. F. Silva, D. R. Austin, A. Thai, M. Baudisch, M. Hemmer, D. Faccio, A. Couairon, and J. Biegert, "Multi-octave supercontinuum generation from mid-infrared filamentation in a bulk crystal," Nat. Commun. **3**, 807 (2012).
23. E. A. Stepanov, A. A. Lanin, A. A. Voronin, A. B. Fedotov, and A. M. Zheltikov, "Solid-state source of subcycle pulses in the midinfrared," Phys. Rev. Lett. **117**, 043901 (2016).
24. D. Kartashov, S. Ališauskas, A. Pugžlys, A. Voronin, A. Zheltikov, M. Petrarca, P. Béjot, J. Kasparian, J.-P. Wolf, and A. Baltuška, "White light generation over three octaves by femtosecond filament at 3.9 μm in argon," Opt. Lett. **37**, 3456–3458 (2012).
25. C. J. Saraceno, F. Emaury, C. Schriber, M. Hoffmann, M. Golling, T. Südmeyer, and U. Keller, "Ultrafast thin-disk laser with 80 μJ pulse energy and 242 W of average power," Opt. Lett. **39**, 9–12 (2014).
26. J. Brons, V. Pervak, D. Bauer, D. Sutter, O. Pronin, and F. Krausz, "Powerful 100-fs-scale Kerr-lens mode-locked thin-disk oscillator," Opt. Lett. **41**, 3567–3570 (2016).
27. H. Fattahi, A. Alismail, H. Wang, J. Brons, O. Pronin, T. Buberl, L. Vámos, G. Arisholm, A. M. Azzeer, and F. Krausz, "High-power, 1-ps, all-Yb:YAG thin-disk regenerative amplifier," Opt. Lett. **41**, 1126–1129 (2016).
28. G. Cerullo, A. Baltuška, O. Mücke, and C. Vozzi, "Few-optical-cycle light pulses with passive carrier-envelope phase stabilization," Laser Photon. Rev. **5**, 323–351 (2011).
29. A.-L. Calendron, H. Çankaya, G. Cirmi, and F. X. Kärtner, "White-light generation with sub-ps pulses," Opt. Express **23**, 13866–13879 (2015).
30. T. Buberl, A. Alismail, H. Wang, N. Karpowicz, and H. Fattahi, "Self-compressed, spectral broadening of a Yb:YAG thin-disk amplifier," Opt. Express **24**, 10286–10294 (2016).
31. M. Bradler, P. Baum, and E. Riedle, "Femtosecond continuum generation in bulk laser host materials with sub-μJ pump pulses," Appl. Phys. B **97**, 561–574 (2009).
32. P. Tzankov, I. Buchvarov, and T. Fiebig, "Broadband optical parametric amplification in the near UV-VIS," Opt. Commun. **203**, 107–113 (2002).
33. L. Canova, S. Kourtev, N. Minkovski, R. Lopez-Martens, O. Albert, and S. M. Saltiel, "Cross-polarized wave generation in the UV region," Opt. Lett. **33**, 2299–2301 (2008).
34. T.-J. Wang, Z. Major, I. Ahmad, S. A. Trushin, F. Krausz, and S. Karsch, "Ultra-broadband near-infrared pulse generation by noncollinear OPA with angular dispersion compensation," Appl. Phys. B **100**, 207–214 (2010).
35. S.-W. Huang, J. Moses, and F. X. Kärtner, "Broadband noncollinear optical parametric amplification without angularly dispersed idler," Opt. Lett. **37**, 2796–2798 (2012).
36. H. Liang, P. Krogen, R. Grynko, O. Novak, C.-L. Chang, G. J. Stein, D. Weerawarne, B. Shim, F. X. Kärtner, and K.-H. Hong, "Three-octave-spanning supercontinuum generation and sub-two-cycle self-compression of mid-infrared filaments in dielectrics," Opt. Lett. **40**, 1069–1072 (2015).
37. M. Cassataro, D. Novoa, M. C. Günendi, N. N. Edavalath, M. H. Frosz, J. C. Travers, and P. St.J. Russell, "Generation of broadband mid-IR and UV light in gas-filled single-ring hollow-core PCF," Opt. Express **25**, 7637–7644 (2017).